

Performance Analysis of Adaptive Coded Modulation with Antenna Diversity and Feedback Delay

Kjell J. Hole, Henrik Holm, and Geir E. Øien

Abstract

A general adaptive coding scheme for spectrally efficient transmission on flat fading channels was introduced by the authors in an earlier paper [2]. An instance of the coding scheme utilizes a set of multidimensional trellis codes designed for additive white Gaussian noise channels of different qualities. A feedback channel between the decoder and encoder makes it possible for the encoder to switch adaptively between these codes based on channel state information fed back from the decoder. In this paper, the adaptive coding scheme is employed in a mobile wireless communication system consisting of a stationary transmitter with one antenna, a wireless Rayleigh fading channel, and a mobile terminal with one or more receive antennas. The bit-error-rate at the output of the decoder is determined for various terminal speeds, time delays in the feedback channel, and number of receive antennas. The obtained results indicate that the proposed adaptive coding scheme is well suited for communications over mobile wireless channels with carrier frequencies in the high MHz range, delay spread up to 250 ns, and terminal mobility up to pedestrian speed.

I. Introduction

Many authors have studied adaptive (coded) modulation for wireless communications (see [1] and the references therein). In an earlier paper [2], we considered a general adaptive coding scheme for single-user channels with frequency-flat slowly varying multipath fading. A particular instance of this coding scheme utilizes a set of multidimensional trellis codes designed for additive white Gaussian noise (AWGN) channels of different qualities. A feedback channel makes it possible for the encoder to switch adaptively between these codes based on channel state information (CSI) fed back from the decoder, thus resulting in an overall scheme with high spectral efficiency.

The output bit-error-rate (BER) of an adaptive coding scheme may increase with growing time delay in the feedback channel and/or increasing terminal speed [3]. Since any implemented feedback channel has nonzero feedback delay, and since it is necessary to allow for mobile terminals, it is important to determine the BER degradation of the proposed adaptive coding scheme in [2]. Alouini and Goldsmith [4] have determined the BER degradation for *uncoded* adaptive modulation. In this paper, we extend their technique to determine the BER degradation of any instance of the proposed adaptive coding scheme.

We first introduce, in Section II, a mobile wireless channel with Rayleigh fading, where the mobile terminal has multiple receive antennas whose signals are combined using the *maximal ratio combining* (MRC) method [5, Ch. 5]. For any instance of the adaptive coding scheme and any number of receive antennas, Section III then shows how to determine the BER degradation associated with a nonzero feedback delay and a nonzero terminal speed. As an example, Section

The authors are with the Department of Telecommunications, Norwegian University of Science and Technology, O. S. Bragstads plass 2B, N-7491 Trondheim, Norway. K. J. Hole is also with the Department of Informatics, University of Bergen, HiB, N-5020 Bergen, Norway (e-mail: Kjell.Hole@ii.uib.no, {Henrik.Holm,Geir.Oien}@tele.ntnu.no).

IV evaluates a specific adaptive encoder and decoder (codec) utilizing a set of four-dimensional trellis codes. A conclusion is drawn in Section V.

II. System model and coding scheme

The system model consists of a stationary transmitter/receiver (transceiver), a wireless frequency-flat fading channel, and a mobile transceiver, or terminal. It is assumed that the distance between the stationary transceiver and the mobile terminal is not more than a few hundred meters. We will only consider the flow of user information on the downlink. Hence, in our model the *feedback channel* (or uplink) from the terminal to the receiver will only be used for CSI.

The stationary transceiver has one transmit antenna, while the mobile terminal has $H (\geq 1)$ receive antennas. Each of the H antenna branches is modeled as a Rayleigh fading channel with ideal coherent detection. It is assumed that the branch signals are statistically independent.

Denoting the transmitted complex baseband signal at time index $t \in \{0, 1, 2, \dots\}$ by $x(t)$, the received signal at antenna $h \in \{1, 2, \dots, H\}$ can then be written as $y_h(t) = \alpha_h(t) \cdot x(t) + n_h(t)$. Here, the stationary and ergodic *fading envelope* $\alpha_h(t)$ is a real-valued random variable with a Rayleigh distribution, and $n_h(t)$ is complex-valued AWGN with statistically independent real and imaginary components. The total one-sided power spectral density of the AWGN is denoted N_0 [W/Hz] and the one-sided channel bandwidth is denoted B [Hz].

Let S [W] denote the constant average transmit power. The instantaneous received *carrier-to-noise ratio* (CNR) on antenna branch h at time index t is then

$$\gamma_h(t) = \frac{\alpha_h^2(t) \cdot S}{N_0 B}, \quad h = 1, 2, \dots, H,$$

with expectation $E[\gamma_h(t)] = \bar{\gamma}_h = \Omega S / (N_0 B)$ where $\Omega = E[\alpha_h^2(t)]$ is assumed independent of h . Thus, $\bar{\gamma}_h$ is also equal for all h .

The mobile terminal implements an MRC combiner to process the H received branch signals [5, p. 316].

Since the branch signals are statistically independent, the instantaneous CNR at the output of the H -branch MRC combiner is given by $\gamma = \sum_{h=1}^H \gamma_h$.¹ If we denote $E[\gamma] = \bar{\gamma}$, then $\bar{\gamma}_h = \bar{\gamma}/H$, and the *gamma* probability density function (pdf) of the instantaneous CNR γ at the output of the MRC combiner may be written as [5, Eq. (5.2-14)]

$$p_\gamma(\gamma) = \left(\frac{H}{\bar{\gamma}}\right)^H \frac{\gamma^{H-1}}{(H-1)!} \exp\left(-H\frac{\gamma}{\bar{\gamma}}\right), \quad \gamma \geq 0. \quad (1)$$

It is convenient to view the combination of the H antenna branches and the MRC combiner as a single channel. The instantaneous CNR γ at the output of this channel determines the *channel state* at a given time. We assume that the mobile terminal has perfect knowledge of γ . The range $[0, \infty)$ of possible CNR values is divided into $N + 1$ nonoverlapping intervals (or *fading regions*). At any given time the CNR will fall in one of these fading regions, and the associated CSI, i.e. the region index $n \in \{0, 1, \dots, N\}$, is sent to the stationary receiver via the feedback channel, which is assumed to be error free.

Assume that $\gamma \in [0, \gamma_1)$ in fading region 0, $\gamma \in [\gamma_n, \gamma_{n+1})$ in region $n \in \{1, 2, \dots, N-1\}$, and $\gamma \in [\gamma_N, \infty)$ in region N . Also, assume that the BER must never exceed a target maximum BER_0 . When $\gamma \in [\gamma_n, \gamma_{n+1})$ we use a multidimensional trellis code, denoted code $n \in \{1, 2, \dots, N\}$, designed to achieve a $\text{BER} \leq \text{BER}_0$ on an AWGN channel of CNR $\gamma \geq \gamma_n$. For $\gamma < \gamma_1$, i.e. γ in fading region 0, the channel conditions are so bad that no information is transmitted, and we have an *outage* during which the information flow is buffered.

Let $4 \leq M_1 < M_2 < \dots < M_N$ denote the number of symbols in N quadrature amplitude modulation (QAM) constellations of growing size, and let code n be based on the constellation with M_n symbols. For some small fixed $L \in \{1, 2, \dots\}$, the encoder for code n accepts $L \cdot \log_2(M_n) - 1$ information bits at each time index $k = L \cdot t \in \{0, L, 2L, \dots\}$ and generates $L \cdot \log_2(M_n)$ coded bits. The coded bits specify L modulation symbols in the n th QAM constellation. These symbols are transmitted at time indices

¹We suppress the time dependence from now on for notational simplicity.

$k, k+1, \dots, k+L-1$. The L two-dimensional symbols can be viewed as one $2L$ -dimensional symbol, and for this reason the code is said to be a $2L$ -dimensional trellis code. In practice, the N codes are chosen such that they may be encoded and decoded by the same codec [2].

To determine the values of the fading region boundaries (or thresholds) γ_n , we need to determine the BER performance of each code. When code n is operating on an AWGN channel of CNR γ , the BER-CNR relationship for varying γ may be approximated by the expression

$$\text{BER} \approx a_n \cdot \exp\left(\frac{-b_n \gamma}{M_n}\right), \quad (2)$$

where $a_n (> 0)$ and $b_n (> 0)$ are constants which depend only on the weight distribution of the code [2]. These constants can be found for any given code by least-squares curve fitting of data from AWGN channel simulations to (2). The fitting must be done separately for each code in the set.

Plots of BER found in the literature indicate that the approximation in (2) is accurate for any CNR γ resulting in $\text{BER} \lesssim 10^{-1}$ (see Fig. 1 for an example). Unfortunately, for the minimum value $\gamma = 0$, the approximation reduces to $\text{BER} \approx a_n$, and since a_n can be larger than one, (2) may be of little use for low CNRs. When we only want to approximate the BER at moderate-to-high CNRs, as was done in [2], this is not a problem. However, we need to approximate the BER for any CNR $\gamma \geq 0$ in this paper, and we will therefore use the following BER expression for code n

$$\text{BER}_n = \begin{cases} a_n \cdot \exp\left(-\frac{b_n \gamma}{M_n}\right), & \gamma \geq \gamma_n^* \\ \frac{1}{2}, & \gamma < \gamma_n^* \end{cases} \quad (3)$$

Here, the boundary

$$\gamma_n^* = \frac{\ln(2a_n) M_n}{b_n}$$

is the smallest CNR such that the BER is no larger than 0.5. The boundary was obtained by assuming equality in (2), setting $\text{BER} = 0.5$, and solving for γ .

For a true BER between 10^{-1} and 0.5 the exponential expression in (3) tends to produce a larger value

than the true BER, assuming that the coded communication system manages to maintain synchronization. In practice, it is difficult to maintain synchronization for a very high BER, and the approximation $\text{BER} = 0.5$ may therefore be close to the true BER of a real system. If the coded system should exhibit a $\text{BER} > 0.5$ for a very low CNR, then all decoded information bits may be flipped to achieve a $\text{BER} < 0.5$. Hence, 0.5 is a reasonable upper bound on the BER.

Assuming a target BER_0 such that $\gamma > \gamma_n^*$ and setting BER_n equal to BER_0 in (3), the thresholds are given by [2]

$$\begin{aligned} \gamma_n &= (M_n K_n)/b_n, & n = 1, 2, \dots, N \\ \gamma_{N+1} &= \infty \end{aligned} \quad (4)$$

where $K_n = -\ln(\text{BER}_0/a_n)$.

The probability that γ falls in fading region n , $P_n = P(\gamma_n \leq \gamma < \gamma_{n+1})$, is given by [4, Eq. (10)]

$$P_n = \frac{\Gamma\left(H, \frac{H\gamma_n}{\gamma}\right) - \Gamma\left(H, \frac{H\gamma_{n+1}}{\gamma}\right)}{(H-1)!} \quad (5)$$

where

$$\Gamma(v, \mu) = \int_{\mu}^{\infty} t^{v-1} e^{-t} dt \quad (6)$$

is the *complementary incomplete gamma function* [6, Eq. (8.350.2)]. Since H is an integer in (5), the function may be calculated using [6, Eq. (8.352.2)].

III. BER degradation

The BER degradation due to nonzero feedback delay and nonzero terminal speed is determined in this section. It is assumed that the communication system utilizes a set of N trellis codes with known parameters a_n and b_n .

Let the *total feedback delay*, τ [s] be the time between the moment the mobile terminal acquires a set of L modulation symbols and the moment the stationary transmitter activates a new code. The total feedback delay is determined by the sum of three delays: i) the processing time needed by the terminal to estimate the instantaneous CNR γ and to determine in which fading region n the CNR falls, ii) the time needed to feed back the region index n to the

transmitter, and iii) the processing time needed by the transmitter to activate code n .

In a real system, the processing delay i) depends on the technique used to estimate the instantaneous received CNR, whereas the processing delay iii) depends on the encoder complexity. Since the distance between the stationary transceiver and the mobile terminal is assumed to be no more than a few hundred meters, the transmission delay ii) is mainly determined by the communication protocols.

The size of the signal constellation $M_n = M_n(\gamma)$ at time index t is a function of the instantaneous received CNR γ , but the constellation is used at time $t+\tau$ when γ has changed to γ_τ . Consequently, while the CNR γ falls in some fading region n , i.e. $\gamma_n \leq \gamma < \gamma_{n+1}$, the CNR γ_τ may fall outside this region. Substituting γ_τ for γ in (3), we can write the BER as a function of γ_τ for a given γ :

$$\text{BER}_n^\tau(\gamma_\tau|\gamma) = \begin{cases} a_n \cdot \exp\left(-\frac{b_n \gamma_\tau}{M_n(\gamma)}\right), & \gamma_\tau \geq \gamma_n^* \\ \frac{1}{2}, & \gamma_\tau < \gamma_n^* \end{cases} \quad (7)$$

The average BER for γ in fading region n is now given by

$$\langle \text{BER} \rangle_n^\tau = \int_{\gamma_n}^{\gamma_{n+1}} \left\{ \int_0^\infty \text{BER}_n^\tau(\gamma_\tau|\gamma) p_{\gamma_\tau|\gamma}(\gamma_\tau|\gamma) d\gamma_\tau \right\} p_\gamma(\gamma) d\gamma, \quad (8)$$

where $p_\gamma(\gamma)$ is given by (1). Furthermore, $p_{\gamma_\tau|\gamma}(\gamma_\tau|\gamma)$ is the pdf of γ_τ conditioned on γ [4]

$$p_{\gamma_\tau|\gamma}(\gamma_\tau|\gamma) = \frac{H}{(1-\rho)\bar{\gamma}} \left(\frac{\gamma_\tau}{\rho\gamma} \right)^{(H-1)/2} \cdot I_{H-1} \left(\frac{2H\sqrt{\rho\gamma\gamma_\tau}}{(1-\rho)\bar{\gamma}} \right) \cdot \exp\left(-\frac{H(\rho\gamma + \gamma_\tau)}{(1-\rho)\bar{\gamma}}\right). \quad (9)$$

The function $I_{H-1}(\cdot)$ in (9) is the $(H-1)$ th-order modified Bessel function of the first kind [7, Ch. 9]. The pdf also contains the channel power correlation coefficient ρ at lag τ . It is shown in Appendix A that ρ is given by the square of the zeroth-order Bessel

function of the first kind [7, Ch. 9],

$$\rho = J_0^2(2\pi f_D \tau), \quad (10)$$

for any number of receive antennas. Here, $f_D = v/\lambda$ [Hz] is the maximum Doppler frequency shift defined by the terminal speed v [m/s] and the wavelength λ [m] of the carrier.

Using (7), the average BER in fading region n given by (8) can be rewritten as the difference between two double integrals,

$$\langle \text{BER} \rangle_n^\tau = \mathcal{I}1(n) - \mathcal{I}2(n),$$

where

$$\mathcal{I}1(n) \stackrel{\text{def}}{=} \int_{\gamma_n}^{\gamma_{n+1}} \left\{ \int_0^\infty a_n \cdot \exp\left(-\frac{b_n \gamma_\tau}{M_n}\right) p_{\gamma_\tau|\gamma}(\gamma_\tau|\gamma) d\gamma_\tau \right\} \cdot p_\gamma(\gamma) d\gamma \quad (11)$$

and

$$\mathcal{I}2(n) \stackrel{\text{def}}{=} \int_{\gamma_n}^{\gamma_{n+1}} \left\{ \int_0^{\gamma_n^*} \left[a_n \cdot \exp\left(-\frac{b_n \gamma_\tau}{M_n}\right) - \frac{1}{2} \right] p_{\gamma_\tau|\gamma}(\gamma_\tau|\gamma) d\gamma_\tau \right\} \cdot p_\gamma(\gamma) d\gamma. \quad (12)$$

The double integral $\mathcal{I}2(n)$ is zero for $\gamma_n^* = 0$, i.e., when parameters a_n and b_n result in good BER approximations for any $\gamma_\tau \geq 0$. Hence, $\mathcal{I}2(n)$ may be viewed as a ‘‘correction term’’ needed when a_n and b_n are only useful for $\gamma_\tau \geq \gamma_n^* > 0$.

It is shown in Appendix B that

$$\mathcal{I}1(n) = \frac{a_n}{(H-1)!} \left(\frac{H}{\bar{\gamma}} \right)^H \frac{\Gamma(H, \beta_n \gamma_n) - \Gamma(H, \beta_n \gamma_{n+1})}{(\omega_n)^H} \quad (13)$$

where

$$\beta_n = \frac{H}{\bar{\gamma}} + \frac{H\rho b_n}{HM_n + \bar{\gamma}(1-\rho)b_n} \quad (14)$$

and

$$\omega_n = \frac{H}{\bar{\gamma}} + \frac{b_n}{M_n}. \quad (15)$$

From Appendix C, we have

$$\mathcal{I}2(n) = \mathcal{S}(a_n, b_n) - \mathcal{S}(\frac{1}{2}, 0) \quad (16)$$

for

$$\begin{aligned} \mathcal{S}(a_n, b_n) &\stackrel{\text{def}}{=} a_n \frac{(1-\rho)^H}{(H-1)!} \\ &\cdot \left\{ \sum_{j=0}^{\infty} \frac{\rho^j}{(j+H-1)! j!} \left[\frac{HM_n}{b_n(1-\rho)\bar{\gamma} + HM_n} \right]^{j+H} \right. \\ &\cdot \gamma_{\text{inc}} \left(H+j, \left[\frac{b_n}{M_n} + \frac{H}{(1-\rho)\bar{\gamma}} \right] \gamma_n^* \right) \\ &\cdot \left. \left[\Gamma \left(H+j, \frac{H\gamma_n}{(1-\rho)\bar{\gamma}} \right) - \Gamma \left(H+j, \frac{H\gamma_{n+1}}{(1-\rho)\bar{\gamma}} \right) \right] \right\}, \end{aligned} \quad (17)$$

where

$$\gamma_{\text{inc}}(v, \mu) = \int_0^{\mu} t^{v-1} e^{-t} dt \quad (18)$$

is the *incomplete gamma function* [6, Eq. (8.350.1)]. Since $H+j$ is an integer in (17), the function may be calculated using [6, Eq. (8.352.1)].

The average BER over all N codes, denoted by $\langle \text{BER} \rangle^\tau$, is equal to the expected number of information bits in error per modulation symbol divided by the expected number of transmitted information bits per modulation symbol,

$$\begin{aligned} \langle \text{BER} \rangle^\tau &= \frac{\sum_{n=1}^N i_n \langle \text{BER} \rangle_n^\tau}{\sum_{n=1}^N i_n P_n} \\ &= \frac{\sum_{n=1}^N i_n [\mathcal{I}1(n) - \mathcal{I}2(n)]}{\sum_{n=1}^N i_n P_n}. \end{aligned} \quad (19)$$

Here, $i_n = \log_2(M_n) - 1/L$ is the number of information bits per modulation symbol and P_n is defined by (5). In practice, the double integral $\mathcal{I}2(n)$ can only be approximated since the sum in (17) must be terminated after a finite number of terms. Since each term in the sum is positive, the termination causes the expression in (19) to become an upper bound on the BER. The tightness of the bound improves as the number of terms is increased. We will use the ten first terms in the sum of (17) in the next section.

IV. Evaluation of example codec

An adaptive codec with eight 4-dimensional trellis codes was described in [2]. The individual codes'

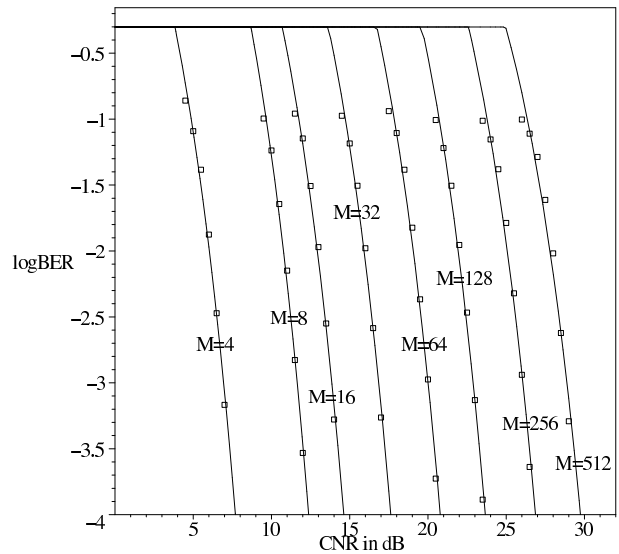


Figure 1: The boxes are BER estimates generated by software simulation and the curves are estimates obtained from (3). The labels indicate the number of symbols in the QAM signal constellations utilized by the 4-dimensional trellis codes.

BER performances on an AWGN channel were simulated for various CNRs. The obtained BER points (represented by boxes) are shown in Fig. 1. Curve fitting with the least squares method was used to obtain the parameters a_n and b_n listed in Table 1. The corresponding BER approximations (3) are plotted in Fig. 1. The expression in (4) was used to determine the tabulated thresholds² γ_n (rounded to one decimal digit) for target $\text{BER}_0 = 10^{-4}$.

Using the thresholds γ_n , setting $L = 2$, and $\bar{\gamma}_h = 20$ dB, the base-10 logarithm of the average BER (19) is plotted as a function of the correlation coefficient ρ in Fig. 2 for $H \in \{1, 2, 4\}$ receive antennas. We observe that because the thresholds are chosen according to (4), the instantaneous BER is smaller than the target BER_0 for $\gamma_n < \gamma < \gamma_{n+1}$ and ρ close to one. As a result, the average BER will be below BER_0 for large ρ (see Fig. 2).

²The thresholds in Table 1 are larger than the thresholds in [2, Table I] because we have reduced the target BER_0 from 10^{-3} to 10^{-4} . Furthermore, the path memory length of the Viterbi decoder was set to 9 in [2] while a path memory length of 16 was used in this paper.

n	M_n	a_n	b_n	γ_n [dB] \approx
1	4	188.7471	9.8182	7.7
2	8	288.8051	6.8792	12.4
3	16	161.6898	7.8862	14.6
4	32	142.6920	7.8264	17.6
5	64	126.2118	7.4931	20.8
6	128	121.5189	7.7013	23.7
7	256	79.8360	7.1450	26.9
8	512	34.6128	6.9190	29.7

Table 1: Parameters a_n and b_n for example codec and calculated thresholds γ_n [dB] for target $\text{BER}_0 = 10^{-4}$.

H	min. ρ	τ_{\max} [ms] \approx	τ_{\max}/T [symb.] \approx
1	0.997	2.7	1,080
2	0.991	3.4	1,360
4	0.963	6.9	2,760

Table 2: Minimum correlation coefficient ρ needed to achieve $\text{BER} \leq 10^{-4}$ for average antenna branch CNR $\bar{\gamma}_h = 20$ dB and different number H of receive antennas. Maximum tolerable delay τ_{\max} [ms] and number of modulation symbols transmitted during τ_{\max} for carrier frequency 1900 MHz, bandwidth 400 kHz, and terminal speed $v = 1$ m/s.

Let τ_{\max} denote the maximum total delay, or *maximum tolerable delay*, for a given target BER_0 . The expression (10) for ρ can be used to determine the maximum tolerable delay τ_{\max} for different Doppler shifts f_D and targets BER_0 . The minimum values of ρ (rounded to three decimal digits) needed to achieve $\langle \text{BER} \rangle^\tau \leq \text{BER}_0 = 10^{-4}$ are listed in Table 2 for $H \in \{1, 2, 4\}$.

If we let the carrier frequency be $f = 1900$ MHz and use the value $c = 3 \cdot 10^8$ m/s for the speed of light, then the wavelength of the carrier frequency is $\lambda = c/f = 3/19 (\approx 0.16)$ m. A mobile terminal with (pedestrian) speed $v = 1$ m/s then has Doppler shift $f_D = v/\lambda = 19/3 (\approx 6.33)$ Hz. The corresponding maximum tolerable delays τ_{\max} (rounded to one decimal digit) are listed in Table 2.

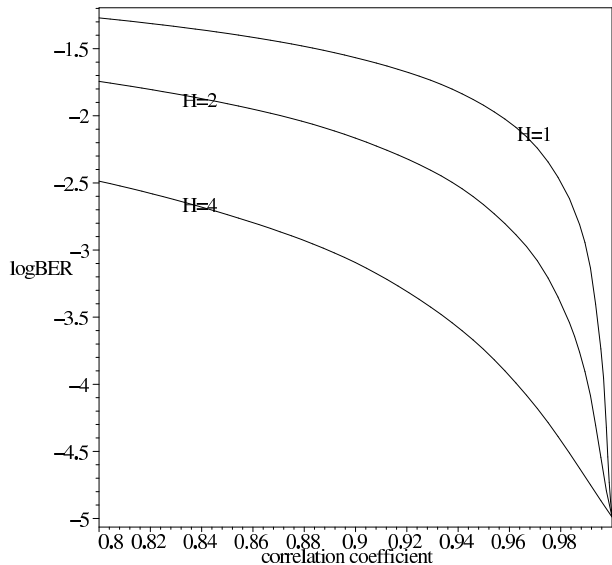


Figure 2: Base-10 logarithm of average BER for correlation coefficient $0.8 \leq \rho < 1$, target $\text{BER}_0 = 10^{-4}$, and average antenna branch CNR $\bar{\gamma}_h = 20$ dB.

To see that the fading is nearly constant over many hundred modulation symbols for communications at pedestrian speed, we calculate the number of symbols transmitted during the maximum tolerable delay τ_{\max} . We first need to determine a bandwidth B for which it is reasonable to assume that the fading is frequency flat. The (rms) *delay spread*, σ_d [s], measures how much a signal component may be delayed during transmission [8, Sec. 2.2.2]. The reciprocal of the delay spread provides a measure of the width of the band of frequencies which are similarly affected by the channel response. The channel is therefore approximately frequency flat if the bandwidth $B \ll 1/\sigma_d$.

At 1900 MHz, the multipath delay spread is up to $\sigma_d = 250$ ns for a cordless phone in indoor and outdoor environments [9]. Hence, we may assume that a channel with bandwidth at least up to $B = 400$ kHz has frequency flat fading. The time needed to transmit one symbol at the Nyquist signaling rate is $T = 1/B = 2.5 \mu\text{s}$, resulting in τ_{\max}/T symbols being transmitted during the maximum tolerable delay. Using the rounded values of τ_{\max} in Table 2, we obtain the τ_{\max}/T values listed in the rightmost column of Table

2 for terminal speed $v = 1$ m/s and $H \in \{1, 2, 4\}$.

V. Conclusion

It has been shown (see Fig. 2) that the BER performance may degrade considerably as ρ decreases, which—for a given carrier frequency—corresponds to increasing the terminal speed. However, the degradation can be mitigated by the use of MRC antenna diversity. Still, our results indicate that adaptive coded modulation may be best suited for systems with moderate mobility requirements, with terminals moving at pedestrian speed.

Appendix A—Calculation of ρ

In this appendix we show that the channel power correlation coefficient ρ is given by the expression in (10). The instantaneous received CNR on the channel may be expressed as $\gamma = \alpha^2 \cdot K$ where α^2 is the channel power gain and $K = S/(N_0 B)$. Since $E[\gamma] = \sum_{h=1}^H E[\gamma_h] = HK\Omega$, we have $E[\alpha^2] = H\Omega$. Assume that α^2 is the power gain at some time t and let α_τ^2 be the power gain at time $t + \tau$ for $\tau > 0$. The correlation coefficient ρ between α^2 and α_τ^2 is then given by

$$\rho = \frac{\text{cov}(\alpha^2, \alpha_\tau^2)}{\sqrt{\sigma_{\alpha^2}^2 \sigma_{\alpha_\tau^2}^2}} = \frac{E[\alpha^2 \alpha_\tau^2] - E[\alpha^2] E[\alpha_\tau^2]}{\sigma_{\alpha^2} \sigma_{\alpha_\tau^2}}. \quad (20)$$

The channel gain α^2 is gamma distributed [8, p. 48]. Hence, assuming that the channel power gains α^2 and α_τ^2 have the same expectations and standard deviations, we have $E[\alpha^2] E[\alpha_\tau^2] = (H\Omega)^2$ and $\sigma_{\alpha^2} \sigma_{\alpha_\tau^2} = (E[\alpha^2])^2/H = H\Omega^2$ in (20).

To calculate $E[\alpha^2 \alpha_\tau^2]$, we first compare two different expressions for the instantaneous received CNR γ . When the communication channel is viewed as a Rayleigh fading channel with a H -branch MRC combiner, then $\gamma = \sum_{h=1}^H \gamma_h = K \sum_{h=1}^H \alpha_h^2$ where α_h^2 is the power gain on the H th antenna branch. Since we also have $\gamma = \alpha^2 \cdot K$, it follows that $\alpha^2 = \sum_{h=1}^H \alpha_h^2$, and we can write

$$E[\alpha^2 \alpha_\tau^2] = E \left[\left(\sum_{h=1}^H \alpha_h^2 \right) \left(\sum_{i=1}^H \alpha_{i,\tau}^2 \right) \right]$$

$$= \sum_{h=1}^H E[\alpha_h^2 \alpha_{h,\tau}^2] + \sum_{h=1}^H \sum_{i \neq h} E[\alpha_h^2 \alpha_{i,\tau}^2]. \quad (21)$$

Furthermore, because the signals on different antenna branches ($h \neq i$) are statistically independent, the covariance

$$\text{cov}(\alpha_h^2, \alpha_{i,\tau}^2) = E[\alpha_h^2 \alpha_{i,\tau}^2] - E[\alpha_h^2] E[\alpha_{i,\tau}^2] = 0,$$

or equivalently, $E[\alpha_h^2 \alpha_{i,\tau}^2] = \Omega^2$. The expression in (21) is then equal to

$$E[\alpha^2 \alpha_\tau^2] = H E[\alpha_h^2 \alpha_{h,\tau}^2] + H(H-1)\Omega^2,$$

and the correlation coefficient in (20) reduces to

$$\rho = \frac{E[\alpha_h^2 \alpha_{h,\tau}^2] - \Omega^2}{\Omega^2}. \quad (22)$$

Observe that (22) is independent of the number of receive antennas H . In fact, (22) defines the correlation coefficient for a Rayleigh fading channel (without MRC). It is shown in [8, Eq. (2.68)] that the numerator in (22) is equal to $\Omega^2 J_0^2(2\pi f_D \tau)$, and as a result, ρ is given by the expression in (10).

Appendix B—Evaluation of $\mathcal{I}1(n)$

In the following we calculate the double integral in (11). For the inner integral, BER_n in (3) is fixed since the CNR γ is fixed. It follows from (3) that

$$M_n = -\frac{b_n \gamma}{\ln(\text{BER}_n/a_n)}.$$

Using this expression for M_n and setting $D_n = -\ln(\text{BER}_n/a_n)$, the inner integral in (11) is equal to

$$\begin{aligned} \mathcal{I}1(n, \gamma) &\stackrel{\text{def}}{=} a_n \int_0^\infty \frac{H}{(1-\rho)\bar{\gamma}} \left(\frac{\gamma_\tau}{\gamma\rho} \right)^{(H-1)/2} \\ &\cdot \exp \left(-\frac{H(\rho\gamma + \gamma_\tau)}{(1-\rho)\bar{\gamma}} - \frac{D_n \gamma_\tau}{\gamma} \right) \\ &\cdot I_{H-1} \left(\frac{2H\sqrt{\rho\gamma\gamma_\tau}}{\bar{\gamma}(1-\rho)} \right) d\gamma_\tau. \end{aligned} \quad (23)$$

Introducing the constant

$$x = \frac{\rho H^2 \gamma^2}{\bar{\gamma}(1-\rho)(H\gamma + \bar{\gamma}(1-\rho)D_n)}$$

and making the substitution

$$z = \left(\frac{H}{\bar{\gamma}(1-\rho)} + \frac{D_n}{\gamma} \right) \gamma \tau,$$

the integral (23) can be written as

$$\begin{aligned} \mathcal{I}1(n, \gamma) &= a_n \left(\frac{H\gamma}{H\gamma + \bar{\gamma}(1-\rho)D_n} \right)^H \\ &\cdot \exp \left(-\frac{\rho D_n H \gamma}{H\gamma + \bar{\gamma}(1-\rho)D_n} \right) \\ &\cdot \int_0^\infty \left(\frac{z}{x} \right)^{(H-1)/2} e^{-z-x} I_{H-1}(2\sqrt{xz}) dz. \end{aligned} \quad (24)$$

The value of the integral in (24) is equal to $Q_H(x, 0)$ where $Q_H(\cdot, \cdot)$ is the *generalized Marcum Q-function of order H* [7, Eq. (11.63)]. Since $Q_H(x, 0) = Q_1(x, 0) = 1$ for all x , we have

$$\begin{aligned} \mathcal{I}1(n, \gamma) &= a_n \left(\frac{H\gamma}{H\gamma + \bar{\gamma}(1-\rho)D_n} \right)^H \\ &\cdot \exp \left(-\frac{\rho D_n H \gamma}{H\gamma + \bar{\gamma}(1-\rho)D_n} \right). \end{aligned} \quad (25)$$

The double integral in (11) can now be written as

$$\mathcal{I}1(n) = \mathcal{F}(\gamma_n) - \mathcal{F}(\gamma_{n+1}) \quad (26)$$

for

$$\mathcal{F}(\xi) = \int_\xi^\infty \mathcal{I}1(n, \gamma) p_\gamma(\gamma) d\gamma.$$

To calculate $\mathcal{F}(\xi)$, we first observe that BER_n in (3) is no longer a constant since γ varies. Using the connection $D_n = -\ln(\text{BER}_n/a_n) = (b_n\gamma)/M_n$, it follows from (1) and (25) that

$$\begin{aligned} \mathcal{F}(\xi) &= \frac{a_n}{(H-1)!} \left(\frac{H}{\bar{\gamma}} \right)^H \left(\frac{HM_n}{HM_n + \bar{\gamma}(1-\rho)b_n} \right)^H \\ &\cdot \int_\xi^\infty \gamma^{H-1} \exp(-\beta_n\gamma) d\gamma \end{aligned}$$

where β_n is defined by (14). Substituting $t = \beta_n\gamma$ and observing that

$$\left(\frac{HM_n}{HM_n + \bar{\gamma}(1-\rho)b_n} \right)^H \left(\frac{1}{\beta_n} \right)^H = \left(\frac{1}{\omega_n} \right)^H$$

for ω_n defined by (15), we get

$$\mathcal{F}(\xi) = \frac{a_n}{(H-1)!} \left(\frac{H}{\bar{\gamma}} \right)^H \frac{\Gamma(H, \beta_n\xi)}{(\omega_n)^H} \quad (27)$$

where $\Gamma(\cdot, \cdot)$ is given by (6). The expression for $\mathcal{I}1(n)$ in (13) is now obtained from (26) and (27).

Appendix C—Evaluation of $\mathcal{I}2(n)$

We shall calculate the double integral $\mathcal{I}2(n)$ defined by (12). We first split the double integral in two to obtain

$$\begin{aligned} \mathcal{I}2(n) &= \\ &\int_{\gamma_n}^{\gamma_{n+1}} \left\{ \int_0^{\gamma_n^*} a_n \cdot \exp \left(-\frac{b_n\gamma\tau}{M_n} \right) p_{\gamma_\tau|\gamma}(\gamma_\tau|\gamma) d\gamma_\tau \right\} \\ &\cdot p_\gamma(\gamma) d\gamma \end{aligned} \quad (28)$$

$$- \int_{\gamma_n}^{\gamma_{n+1}} \left\{ \int_0^{\gamma_n^*} 2^{-1} p_{\gamma_\tau|\gamma}(\gamma_\tau|\gamma) d\gamma_\tau \right\} p_\gamma(\gamma) d\gamma. \quad (29)$$

The second integral (29) is a special case of the first integral (28) with $a_n = 2^{-1}$ and $b_n = 0$. Hence, we only need to consider the first integral. The pdf $p_{\gamma_\tau|\gamma}(\gamma_\tau|\gamma)$ defined by (9) contains the $(H-1)$ th-order modified Bessel function of the first kind defined by [7, Eq. (9.28)]

$$I_\nu(z) = \left(\frac{1}{2}z \right)^\nu \sum_{j=0}^{\infty} \frac{(\frac{1}{2}z)^{2j}}{(j+\nu)! j!}$$

for ν an integer. Using this definition, the inner integral in (28) is equal to

$$\begin{aligned} &a_n \left[\frac{HM_n}{b_n(1-\rho)\bar{\gamma} + HM_n} \right]^H \cdot \exp \left(-\frac{H\rho\gamma}{(1-\rho)\bar{\gamma}} \right) \\ &\sum_{j=0}^{\infty} \frac{1}{(j+H-1)! j!} \left[\frac{M_n H^2 \rho \gamma}{(1-\rho)\bar{\gamma} \{ b_n(1-\rho)\bar{\gamma} + HM_n \}} \right]^j \\ &\gamma_{\text{inc}} \left(H+j, \left[\frac{b_n}{M_n} + \frac{H}{(1-\rho)\bar{\gamma}} \right] \gamma_n^* \right) \end{aligned}$$

where $\gamma_{\text{inc}}(\cdot, \cdot)$ is defined by (18). The outer integral in (28) is then equal to (17). Since the double integral in (29) is a special case of the double integral in (28), the “correction term” $\mathcal{I}2(n)$ is now given by (16).

References

- [1] K. J. Hole and G. E. Oien, “Spectral efficiency of adaptive coded modulation in urban microcellular networks,” *IEEE Trans. Veh. Technol.*, vol. 50, pp. 1–18, Jan. 2001.

- [2] K. J. Hole, H. Holm, and G. E. Øien, “Adaptive multidimensional coded modulation over flat fading channels,” *IEEE J. Select. Areas Commun.*, vol. 18, pp. 1153–1158, July 2000.
- [3] D. L. Goeckel, “Adaptive coding for time-varying channels using outdated fading estimates,” *IEEE Trans. Commun.*, vol. 47, pp. 844–855, June 1999.
- [4] M.-S. Alouini and A. J. Goldsmith, “Adaptive M-QAM modulation over Nakagami fading channels,” *Proc. 6th Communications Theory Mini-Conference (CTMC VI) in conjunction with IEEE Global Communications Conference (GLOBECOM’97)* (Phoenix, Arizona, Nov. 1997), pp. 218–223.
- [5] W. C. Jakes, Editor, *Microwave Mobile Communications*. Piscataway, NJ: IEEE Press, second ed., 1994.
- [6] I. S. Gradshteyn and I. M. Ryzhik, *Table of Integrals, Series, and Products*. San Diego, CA: Academic Press, fifth ed., 1994.
- [7] N. M. Temme, *Special Functions—An Introduction to the Classical Functions of Mathematical Physics*. New York, NY: John Wiley & Sons, 1996.
- [8] G. L. Stüber, *Principles of Mobile Communication*. Norwell, MA: Kluwer Academic Publishers, 1996.
- [9] T. Ue, S. Sampei, N. Morinaga, and K. Hamaguchi, “Symbol rate and modulation level-controlled adaptive modulation/TDMA/TDD system for high-bit-rate wireless data transmission,” *IEEE Trans. Veh. Technol.*, vol. 47, pp. 1134–1147, Nov. 1998.